

Expression of the p75 TNF Receptor Is Linked to TNF-Induced NFκB Translocation and Oxyradical Neutralization in Glial Cells*

Joel M. Dopp,¹ Theodore A. Sarafian,² Francesca M. Spinella,¹ Michelle A. Kahn,¹ Hungyi Shau,³ and Jean de Vellis^{1,4}

(Accepted June 5, 2002)

Tumor necrosis factor (TNF)-family cytokines induce reactive oxygen species (ROS) that injure vulnerable populations of brain cells. Among glia, oligodendrocytes are particularly susceptible to TNF-induced ROS whereas microglia are protected. We previously found that oligodendrocytes in vitro predominantly express the p55 type-1 TNF receptor, while microglial cells express both type-1 and p75 type-2 receptors. We hypothesized that differential TNF receptor expression and attendant signaling underlies the relative vulnerability of oligodendrocytes, versus microglia, to TNF-induced injury. To test this hypothesis, purified cultures of glial cells were incubated 0–48 hr with TNFα or lymphotoxin-alpha, following which levels of ROS, glutathione (GSH), nuclear factor kappa-B (NFκB) translocation, and anti-oxidant proteins and activity were measured. 48 hr exposure to TNF increased ROS levels 28% and decreased GSH levels 17% in oligodendrocytes, but decreased levels ROS levels 24% and increased GSH levels 112% increase in microglia. Thirty to 180 min exposure to TNF increased NFκB nuclear translocation to a greater extent and for a longer time in microglia versus oligodendrocytes, and this was followed 24–48 hr later with 3- to 13-fold increases in microglia manganese superoxide dismutase protein levels and 6-fold increases in enzyme activity. Collectively, these data suggest that signals transduced through the p75 receptor activate anti-oxidant mechanisms that protect microglia from TNF-induced injury. Lacking such signals, oligodendrocytes are considerably more vulnerable to the injurious effects of TNF.

KEY WORDS: TNF; NFκB; Mn SOD; ROS; microglia; oligodendrocytes.

INTRODUCTION

Cytokines in the tumor necrosis factor family are potent proinflammatory agents implicated in the patho-

genesis of central nervous system (CNS) demyelinating diseases. For example, tumor necrosis factor-alpha (TNFα) is localized to astrocytes and microglia (1), and lymphotoxin-alpha (LTα) is localized to T-cells (2) in active multiple sclerosis (MS) lesions. TNFα injections exacerbate the clinical severity of experimental allergic encephalomyelitis (EAE) (3), an animal model of MS, whereas antibodies against either TNFα (4,5) or soluble type-1 TNF receptors ameliorate EAE (6). TNF

* Special issue in honor of Dr. Juana Maria Pasquini.

¹ Mental Retardation Research Center, University of California at Los Angeles, Los Angeles, California, 90024-1759.

² Department of Medicine, University of California at Los Angeles, Los Angeles, California, 90024-1759.

³ Division of Surgical Oncology, University of California at Los Angeles, Los Angeles, California, 90024-1759.

⁴ Address reprint requests to: Jean de Vellis, University of California at Los Angeles MRRC, 68-177 NPI, 760 Westwood Plaza, Los Angeles, California 90024-1759. Tel: (310) 825-0239; Fax: (310) 206-5061; E-mail: jdevellis@mednet.ucla.edu

Abbreviations: DCF-DA, 2,7-dihydrodichlorofluorescein diacetate; GSH, glutathione; LTα, lymphotoxin-alpha; NFκB, nuclear factor kappa-B; OL, oligodendrocytes; Prx, peroxiredoxin; ROS, reactive oxygen species; SOD, superoxide dismutase; TNFα, tumor necrosis factor-alpha.

ligands (TNF α and LT α) transduce their effects through two primary receptors—the 55-kDa type-1 receptor (TNFR1) and the 75-kDa type-2 receptor (TNFR2)—that have homologous extracellular ligand-binding domains but distinct intracellular domains and divergent signal transduction cascades.

TNF-family cytokines do not affect all types of glial cells uniformly. For example, TNF α stimulates astrocyte proliferation in vitro (7,8) and GFAP upregulation and gliosis in vivo (9). TNF α induces proliferation of microglial cells co-cultured with astrocytes (10–12), and enhances microglia IL-1 β -induced proliferation and IFN γ -induced nitric oxide production (13). In contrast, in oligodendrocytes (OL) it has injurious effects such as altered potassium-channel function (14), inhibition of protein phosphorylation and process extension (15), and demyelination (16). High concentrations of LT α also induce DNA fragmentation and apoptotic cell death in OL (17).

One way that TNF cytokines could differentially affect glial cells is by altering their generation and/or neutralization of reactive oxygen species (ROS). TNF is known to disrupt the electron transport chain in mitochondria (18), initiating the formation of superoxide anions ($\cdot\text{O}_2^-$). Mitochondrial-derived ROS are proposed to be instrumental in initiating apoptosis (19). Scavenger proteins rapidly neutralize potentially harmful ROS, and each protein has a specific intracellular location, metal requirement, and target species. Copper/zinc-dependent superoxide dismutase (Cu/Zn SOD) is located in the cytosol and it catalyzes the conversion of $\cdot\text{O}_2^-$ into hydrogen peroxide (H_2O_2), whereas manganese-dependent SOD (Mn SOD) catalyzes a similar reaction in mitochondria. H_2O_2 is then converted into water by peroxisomal enzymes such as catalase and by cytosolic enzymes such as glutathione peroxidase and peroxiredoxins. Peroxiredoxins are a family of highly conserved anti-oxidant proteins that scavenge not only H_2O_2 but also organic hydroperoxides (20–22). Peroxiredoxins protect cells from apoptosis caused by oxidative damage (23,24) and they are upregulated by oxidants and inflammatory stimuli (22,25,26).

Differential expression of anti-oxidants confers differences among glia in the ability to neutralize ROS. Peroxiredoxins, for example, are differentially expressed among populations of glial cells (27,28). OL precursors also have one third the reduced glutathione (GSH) levels and 23-fold the iron content of astrocytes (29). GSH converts peroxides to water, whereas iron (Fe^{2+}) facilitates the conversion of H_2O_2 into hydroxy radicals ($\cdot\text{OH}$), and lipid hydroperoxides into peroxy radicals. As a result of this disparity, blue light—which excites

molecules such as riboflavin, initiating a cascade that ultimately yields H_2O_2 —induces 17-fold higher ROS levels in OL versus astrocytes (29). Immature OL appear to be most at risk for ROS-induced damage: GSH depletion causes significantly higher levels of ROS and cytotoxicity in pre-OL versus mature, myelin basic protein-expressing cells. ROS-injured OL have chromatin condensation, a decrease in nuclear size, and cytoplasmic vacuolation indicating apoptosis. Early mitochondrial swelling suggests that this organelle is an initiation site of cellular dysfunction (30).

We previously found by Northern and immunocytochemical analyses that rat microglia express both TNFR1 and TNFR2 in vitro, whereas OL predominantly express TNFR1 (12). We hypothesized that differential TNF receptor expression and associated signaling contributes—via differential ROS generation and/or neutralization—to the relative vulnerability of OL to TNF-induced injury. To test this hypothesis, we determined the effects of TNF and LT on levels of ROS, NF κ B translocation, anti-oxidants, and anti-oxidant activity in primary microglia versus OL.

EXPERIMENTAL PROCEDURE

Cell Isolation and Culture. Primary mixed-glia cultures were obtained by slightly modifying the protocol of Cole and de Vellis (31) as previously described (12). Briefly, cerebra from 2-day-old Sprague-Dawley rat pups (B & K Universal, Fremont, CA) were harvested and progenitor cells were cultured at 2×10^6 cells/ml for 5 days. Floating microglia were harvested from 5-day cultures and were 97% acetylated-LDLR $^+$. OL were dissociated from 7- and 8-day astrocyte monolayers by rotational force and plated at 5×10^5 /ml in poly-L-lysine (PLL) (Sigma, St. Louis, MO) coated petri dishes for 2 days before use. Cells were maintained in DNB media containing DMEM (Gibco, Grand Island, NY), N1 supplement (50 $\mu\text{g}/\text{ml}$ transferrin, 5 $\mu\text{g}/\text{ml}$ insulin, 100 mM putrescine, 20 nM progesterone, and 30 nM selenium; Bottenstein et al., 1980), biotin (10 ng/ml), and 0.5% FCS. Basic fibroblast growth factor (bFGF) and platelet-derived growth factor-AA (PDGF-AA) (both 5 ng/ml; both from Boehringer Mannheim; Indianapolis, IN) were added to OL cultures to induce proliferation. When allowed to mature under these conditions for 7–10 days, cultures of OL were 95% galactocerebroside positive.

ROS and GSH Measurement. 2,7-Dihydrodichlorofluorescein diacetate (DCF-DA) was used to measure TNF α -induced ROS following the procedure of Bass et al. (32). DCF-DA diffuses through cell membranes and is deacetylated by intracellular esterases to non-fluorescent DCF-H. In the presence of peroxynitrite, hydrogen peroxide, nitric oxide, or superoxide, DCF-H is converted to highly fluorescent DCF (33). Glial cells were plated at 5×10^4 /100 μl /well in DNB media (described above) in PLL-coated (100 $\mu\text{g}/\text{ml}$) 96-well flat-bottom plates (Corning); 5 ng/ml each of bFGF and PDGF-AA were added to OL. Recombinant rat TNF α (20 ng/ml; Peprotech; Rocky Hill, NJ) was either omitted (control) or added immediately, 24, 36, or 47 hr later; fresh cytokine was added every 24 hr. Hence,

cells were continuously exposed for 0, 1, 12, 24, or 48 hr to TNF. Plates of cells were washed twice with Krebs' Ringer (KR) solution, following which 100 μ l/well 50 mM DCF-DA was added. Plates were sealed with mylar tape and incubated in the dark at room temperature for 20 min. Cells were washed twice with KR to remove unincorporated DCF-DA, and 100 μ M menadione was added to selected wells as a positive control. Fluorescence at 485 nm excitation and 530 nm emission was measured in a Cytofluor 2300 fluorescent plate reader 5, 15, 30, 60 and 120 min later; asymptotic 60-min data were used for analyses. To quantify reduced glutathione (GSH) levels, KR was removed and monochlorobamine (40 μ M in KR) was added to each well. Plates were incubated for 20 min in the dark at 37°C, following which fluorescence at 395 nm excitation and 460 nm emission was measured (34,35). To quantify dead cells, propidium iodide (50 μ M final concentration) was added to each well, plates were incubated in the dark for 15 min, and fluorescence at 530 nm excitation and 590 nm emission was measured. Subsequently, total cell number was quantified by adding digitonin (160 μ M final concentration) to permeabilize cell membranes. Plates were incubated in the dark for 20 min and fluorescence at 530 nm excitation and 590 nm emission was re-measured. To correct for differences among wells in cell number, DCF and GSH data were normalized by dividing them by propidium iodide fluorescence values obtained after digitonin permeabilization.

Western Blots. To measure NF κ B translocation, cells were incubated with 20 ng/ml recombinant rat TNF α (Peprotech) for 0, 30, 60, 120, or 180 min. Cells were washed in ice-cold PBS and cytosolic proteins were harvested by first incubating cells on ice for 15 min in a buffer of 10 mM HEPES, 10 mM KCL, 0.1 mM EDTA, 0.1 mM EGTA, 1 mM DTT, 0.5 mM PMSF, and 1 mM sodium orthovanadate (pH 7.9), then dissolving plasma membranes by the addition of Nonidet P-40 (0.6% final concentration) for 2 min. Lysates were centrifuged for 5 min at 3000 \times g, cytosolic proteins in the supernatant were collected, and nuclei were resuspended and agitated for 30 min on ice in a buffer of 20 mM HEPES, 400 mM NaCl, 1 mM EDTA, 1 mM EGTA, 1 mM DTT, 1mM PMSF, and 1 mM sodium orthovanadate, 1% leupeptin, 1% aprotinin, and 10% glycerol (pH 7.9). Lysates were centrifuged at 12,000 \times g for 10 min and nuclear proteins in the supernatant were collected. To measure TNF-ligand induction of anti-oxidant proteins, glia were incubated with 20 ng/ml recombinant rat TNF α or recombinant human LT α (R & D Systems; Minneapolis, MN; cross reactive with mouse receptors) for 0–48 hr; fresh cytokine was added every 24 hr. Cells were washed in PBS, and total cellular proteins were harvested in a buffer of 200 mM NaCl, 20 mM HEPES, 1 mM MgCl₂, 0.5 mM EDTA, 0.5 mM DTT, protease inhibitors (1mM PMSF, 20 μ g/ml leupeptin, 5 μ g/ml pepstatin, 1 mM sodium orthovanadate, 1 mM iodoacetamide), and 0.1% NP-40 (pH 8.0). Protein concentrations were determined by Bradford assay (Bio-Rad, Hercules, CA), and 100 μ g (anti-oxidant blots) or 50 μ g (NF κ B blots) glial-cell protein, 20 μ g EGF-stimulated A431 carcinoma cell protein, 200 ng bovine Mn SOD, 100 ng rhPrx-II, or 12.5 μ g rat testis protein per lane was electrophoresed for 3 hr in a discontinuous 10% polyacrylamide minigel (Bio-Rad). Separated proteins were transferred for 12 hr at 4°C onto a nitrocellulose membrane (Optitran; Schleicher & Schuell, Keene, NH). Nitrocellulose membranes were blocked for 1 hr in tris-buffered saline (TBS, pH 7.4) containing 3% nonfat dry milk. Blots were washed for 5 min in TBS containing 0.01% Tween-20 (TTBS), and incubated for 1 hr with agitation in TTBS containing one of the following primary antibody solutions: rabbit anti-NF κ B p65 (1:2000, Stressgen; Victoria BC, Canada) sheep anti-Cu/Zn SOD (1:100; Upstate Biotech) and 3% nonfat dry milk; sheep anti-Mn SOD (1:1000; Calbiochem); or

rabbit anti-Prx-I/II (1:1000; polyclonal #628). Rabbit polyclonal antiserum specific for both Prx-I and -II was obtained as previously described (36,37). Blots were washed and incubated for 1 hr in biotinylated rabbit anti-sheep IgG (1:20,000; Vector Labs; Burlingame, CA) or HRP-conjugated goat anti-rabbit IgG (1:40,000; Vector). Blots were washed and protein bands were visualized by enhanced chemiluminescence (Amersham), using exposures of 30 sec to 2 min. Band intensities were determined with ImageQuant software (Molecular Dynamics, Santa Cruz, CA). All Western data were replicated at least once using proteins and blots from independent cultures of glial cells.

SOD Activity Assay. Primary glial cells, cultured as described above in 100-mm² petri dishes, were incubated for 0, 24, or 48 hr with 20 ng/ml recombinant rat TNF α (Peprotech). Cells were washed twice in PBS at room temperature, 500 μ l of 10 mM KPO₄ buffer (pH 7.7) was added to each plate, and cells were removed with a beveled scraper. Cells were homogenized for 2 min in a Dounce homogenizer, alternately freeze/thawed in acetone/dry-ice and 60°C water baths five times, and centrifuged for 3 min at 10,000 \times g; supernatants were stored at –20°C prior to use. Protein concentrations in supernatants were determined via Bradford assay. Into each well of a flat-bottomed 96-well plate was added final concentrations of 10 mM KPO₄ buffer (pH 7.7), 1 mM EDTA, 333 μ g/ml gelatin, 33 μ M PMS, and 375 μ M nitro-blue tetrazolium, with or without 5 mM KCN. 5 μ g protein/sample was added to each well, followed by 1 μ M NADH to initiate the formation of superoxide anion. Color intensity was determined in a Tecan SLT Spectra Shell plate reader 0, 5, 10, and 20 min after the addition of NADH.

Statistics. Paired-sample *t* tests were used to evaluate differences between cell types at various time points or in response to specified treatments.

RESULTS

The DCF assay was used to measure TNF-induced ROS in microglia and OL. To control for inter-assay differences in baseline levels, DCF data were graphed as percent change from baseline. As a point of reference, mean baseline DCF fluorescence values \pm the standard error of the mean (SEM) in unstimulated cells were 1041 \pm 23 for microglia and 572 \pm 52 for OL. As shown in Figure 1, TNF had divergent effects on ROS levels in glia. TNF induced a gradual but consistent increase in OL ROS levels, peaking at 28% above baseline after 48 hr. In contrast, TNF induced a decrease in microglia ROS levels, with values dropping to 20%, 36%, and 24% below baseline after 12, 24, and 48 hr, respectively (all *p* < 0.01).

To investigate mechanisms underlying differences in TNF-induced ROS, we used the monochlorobamine (MCB) assay to determine effects of TNF on levels of GSH. GSH was measured because it both scavenges H₂O₂ via GSH peroxidase and it neutralizes cytotoxic products of lipid peroxidation. Basal levels of MCB fluorescence \pm SEM were 180 \pm 41 for microglia versus

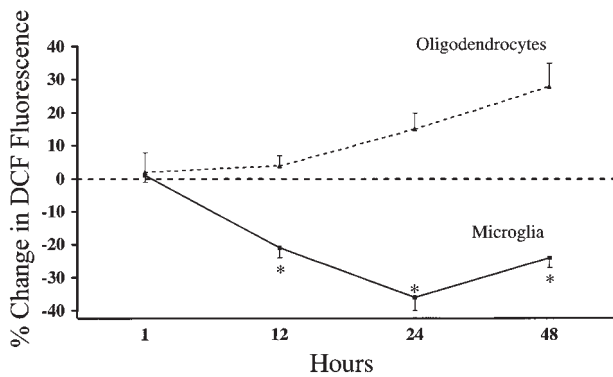


Fig. 1. TNF α increases ROS levels in oligodendrocytes but decreases levels in microglia. Enriched cultures of microglia or oligodendrocytes were incubated for 0–48 hr with 20 ng/ml rat TNF α . Cells were loaded with DCF, washed twice, and incubated in the dark for 20 min. ROS levels were measured 60 min later in a fluorescent plate reader at 485 nm excitation and 530 nm emission. Normalized data are plotted as a percent change from baseline. Each data point represents the mean \pm SEM of 5–14 wells from three independent experiments. Asterisks denote means that differ significantly from the OL mean at the same time point ($p < 0.01$).

118 \pm 15 for OL. Data were again plotted as percent change from baseline. As shown in Figure 2, TNF slightly but consistently decreased GSH levels in OL to 17% below baseline after 48-hr. In contrast, it markedly elevated GSH levels in microglia to 112% above baseline during the same time period ($p < 0.01$), enhancing their anti-oxidant capability.

We used Western blotting to elucidate differences between microglia and OL in TNF-induced signaling and upregulation of anti-oxidant proteins. Figure 3

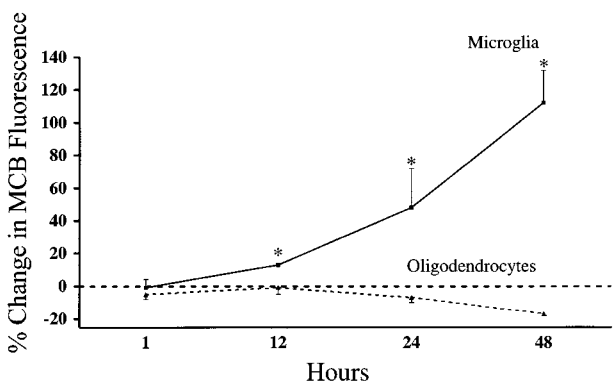


Fig. 2. TNF α decreases GSH levels in oligodendrocytes but increases levels in microglia. Primary glia were plated and treated with TNF α as described in Fig. 1. Following ROS measurement, MCB was used to measure GSH levels at 395 nm excitation and 645 nm emission. Normalized data are plotted as a percent change from baseline. Each data point represents the mean \pm SEM of 5–14 wells from three independent experiments. Asterisks denote means that differ significantly from the OL mean at the same time point ($p < 0.01$).

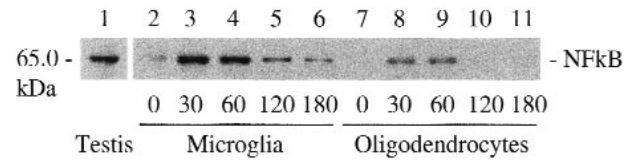


Fig. 3. TNF α -induced p65 NF κ B translocation is stronger and more prolonged in microglia than in oligodendrocytes. Enriched cultures of microglia or oligodendrocytes were incubated for 0–180 min with 20 ng/ml rat TNF α . Nuclear proteins (50 μ g/lane) were electrophoresed through a polyacrylamide gel, transferred onto a nitrocellulose membrane, and probed for the p65 subunit of NF κ B. Protein bands were visualized by enhanced chemiluminescence. Representative data from two independent experiments with similar results are shown.

shows levels of the NF κ B p65 subunit in nuclei of purified microglia and OL. In the absence of TNF, microglia had low nuclear levels of p65 which densitometric analyses indicated were 1.9-fold higher than those in OL. After 30 min exposure to TNF, nuclear levels of p65 in microglia increased to 3.1-fold above baseline, followed by a gradual decline to 2.9- and 1.5-fold increases at 60 and 120 min, and to near baseline levels by 180 min (lanes 2–6 of Fig. 3 and a replicate blot). In contrast, very low baseline levels of p65 in nuclei of OL increased 2.0-, 1.8-, and 1.2-fold 30, 60, and 120 min after the addition of TNF, returning completely to baseline levels by 180 min (lanes 7–11 of Fig. 3 and a replicate blot). As a percentage of baseline, TNF induced 58% and 66% larger increases at 30 and 60 min, respectively, in NF κ B translocation into the nuclei p65 of microglia versus OL. Elevations of nuclear NF κ B above baseline were also more prolonged in microglia, remaining increased for a full 3 hr after exposure to TNF, versus a complete return to baseline in that same period by OL.

To determine whether differences in TNF-induced NF κ B translocation were associated with divergent upregulation of anti-oxidant proteins, we examined effects of TNF and LT α on levels of Cu/Zn SOD, peroxiredoxins, and Mn SOD. Densitometric analyses of Cu/Zn SOD bands (the bottom row in Fig. 4 and a replicate blot) showed that constitutive and induced levels of this protein were approximately 1.7-fold higher in OL versus microglia. However, neither LT nor TNF reliably induced changes in levels of Cu/Zn SOD in either type of cell. Densitometric analyses of peroxiredoxin I and/or II proteins (the middle row of Figure 4 and a replicate blot) indicated that levels were approximately 9.6-fold higher in OL than in microglia. Twenty-four hour exposure to LT increased mean peroxiredoxin levels 86% in microglia, while 48-hr exposure to LT and TNF increased levels 10% and 16%, respectively, in OL. Only mi-

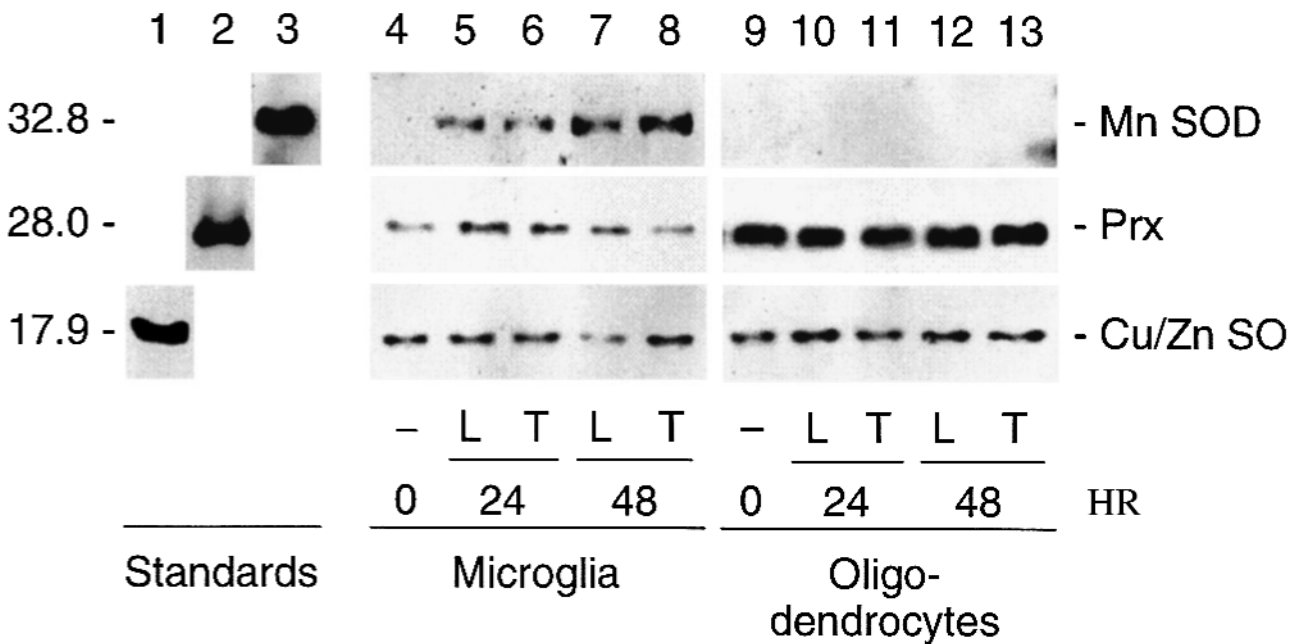


Fig. 4. Microglia and oligodendrocytes differ in constitutive and LT α - or TNF α -induced levels of anti-oxidant proteins. Enriched cultures of microglia or oligodendrocytes were incubated for 0–48 hr with 20 ng/ml LT α (L) or TNF α (T). Total cellular proteins (100 μ g/lane) were electrophoresed through a polyacrylamide gel, transferred onto a nitrocellulose membrane, and probed for Mn SOD or Cu/Zn SOD followed by peroxidase I/II. Protein bands were visualized by enhanced chemiluminescence. Representative data of two independent experiments with similar results are shown.

Microglia expressed detectable levels of Mn SOD (the top row of Fig. 4 and a replicate blot), and incubation with TNF increased levels of this anti-oxidant protein 3.5 and 12.8-fold after 24 and 48-hr, respectively.

To determine whether TNF-induced increases in Mn SOD protein enhanced the ability of microglia to neutralize superoxide anions, we used the nitro-blue tetrazolium assay. This assay detects both Cu/Zn SOD and Mn SOD activity; therefore, potassium cyanide was added to inhibit Cu/Zn SOD activity in selected wells, leaving only the activity of Mn SOD. Figure 5 shows that both microglia and OL expressed low basal levels of Mn SOD enzymatic activity. Corroborating the observed upregulation of Mn SOD protein in Western blots, TNF induced 7- and 5-fold increases in enzymatic activity in microglia by 24 hr and 48 hr, respectively (both $p < 0.05$). Because the majority of this activity could not be inhibited with cyanide (means \pm cyanide were not significantly different at 0, 24, or 48 hr), it is attributable to Mn SOD. In contrast, and again corroborating Western data, TNF did not significantly induce Mn SOD activity in OL.

DISCUSSION

The impetus for this study arose from four convergent lines of published data. First, TNF and LT

induce a reactive, amoeboid phenotype in microglia while causing injury and apoptotic death in OL. Second, we previously found that OL predominantly express TNFR1 whereas microglia express both TNFR1

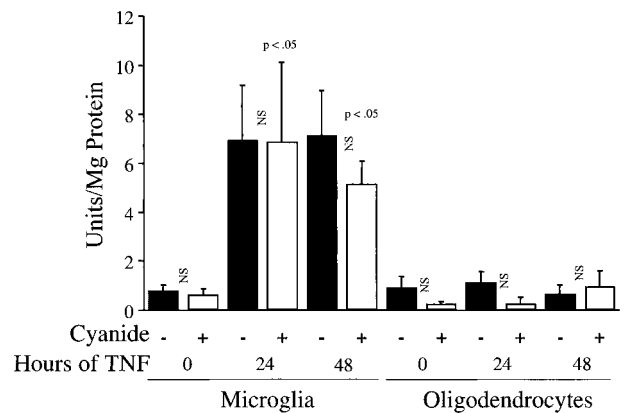


Fig. 5. TNF α increases Mn SOD activity in microglia but not in oligodendrocytes. Enriched cultures of microglia or oligodendrocytes were incubated for 0, 24, or 48 hr with 20 ng/ml rat TNF α . Cell homogenates (5 μ g protein/sample) were treated with nitro-blue tetrazolium, with (+) or without (-) 5 mM KCN, to determine SOD activity. Color intensity was determined in a plate reader 20 min later. Each data point represents the mean \pm SEM of 6 wells from two independent experiments. P values denote means that differ significantly from their baseline at 0 hr. Statistically nonsignificant (NS) differences between the means of wells +/- cyanide are also indicated.

and TNFR2 in vitro. Third, each receptor is linked to a distinct signaling pathway, and TNFR1, is known to induce cleavage of caspases, leading to apoptosis. Finally, TNF increases intracellular ROS levels, and ROS induce OL injury. Integrating these findings, we hypothesized that differential TNFR2 expression is linked—by differential signaling and ROS neutralization—to the divergent effects of TNF on microglia versus OL. Our data support this hypothesis: TNF induced significantly stronger and more prolonged NF κ B translocation, Mn SOD protein upregulation, and Mn SOD enzyme activity in microglia versus OL. We found that OL do express anti-oxidants such as glutathione, Cu/Zn SOD, and peroxiredoxins, but their levels were not increased by TNF nor were they adequate to prevent TNF-induced increases in ROS levels. Elevated ROS levels in mitochondria are critical in initiating TNF-induced apoptosis, and OL are particularly vulnerable to ROS in this organelle. In fact, we detected neither basal nor TNF-induced Mn SOD protein, a key scavenger of mitochondrial ROS, in OL. The net result of differential signaling and anti-oxidant induction is that TNF increases oxyradical levels in OL but has the opposite effect on microglia.

How does differential TNF receptor expression by microglia and OL lead to their dramatically different responses to TNF? Examination of the signaling pathways for the two main receptors provides clues. TNF/receptor binding causes receptor aggregation and subsequent formation of cytoplasmic binding sites for TNF-receptor-associated factors (TRAFs); TRAFs, in turn, activate downstream signaling proteins. TNF/TNFR1 binding activates divergent pathways directly involved in apoptotic cell death. One pathway involves the direct cleavage and activation of a caspase cascade that disrupts cellular structure. The other involves the upregulation of pro-apoptotic proteins through activation of the transcription factor AP-1, and anti-apoptotic proteins through activation of NF κ B. TNF/TNFR2 binding primarily activates the NF κ B pathway. Hence, TNFR1 signals simultaneously induce an apoptotic cascade and a protective NF- κ B cascade, whereas TNFR2 signals primarily induce the protective NF κ B cascade (38,39). Microglia expression of TNFR2 enables them to upregulate protective proteins such as Mn SOD that counteract the apoptotic signals transduced through TNFR1. Lacking TNFR2, OL show less robust and less sustained NF κ B nuclear translocation in response to TNF. Consequently, OL do not activate protective mechanisms and are acutely at risk for TNF-induced oxyradical damage. In fact, the addition of TNF to OL activates interleukin-1 β -converting enzyme (ICE)/

Caenorhabditis elegans-3 (CED-3) and CPP32 proteases, leading to DNA fragmentation and cell death (40).

Based on the above signaling pathways, we hypothesize that TNFR2 signaling in microglia causes strong NF κ B nuclear translocation, resulting in increased transcription/translation of the Mn SOD gene and the increased protein levels and enzymatic activity we observed. This hypothesis is supported by the fact that the Mn SOD promoter contains an NF κ B consensus sequence, and Mn SOD expression in other cells is increased by TNF (41). Constitutive and ROS-induced Mn SOD was previously detected in microglia by immunocytochemistry (42). Our results corroborate and extend these data, showing that Mn SOD protein levels are increased by LT and TNF. Our finding that TNF increases GSH levels in microglia further provides a mechanism whereby harmful H₂O₂—generated by Mn SOD dismutation of $\cdot\text{O}_2^-$ —can be rapidly neutralized.

Mounting evidence indicates that ROS accumulation in mitochondria is critical in initiating apoptosis. Mitochondria are a major source of oxyradicals because 1–5% of electrons escape the respiratory chain and their direct transfer from ubiquinone to molecular oxygen generates superoxide anion (19,43). Increased ROS cause lipid peroxidation in mitochondrial membranes and trigger these organelles to release caspase-activating proteins such as cytochrome *c* (19). Cytochrome *c* enhances cleavage of initiator caspases triggered by TNFR1 signaling, thereby expediting apoptosis. TNFR2 signals strongly induce NF κ B translocation into the nucleus, initiating a protective pathway that counteracts events leading to apoptosis. Protection is inhibited by a dominant-negative I κ B that prevents NF κ B nuclear translocation (44). One important element of this protective pathway is Mn SOD neutralization of mitochondrial ROS, underscoring the significance of our Western data on TNF upregulation of this enzyme in microglia. NF κ B also facilitates upregulation of other protective proteins, including TRAF-1 and TRAF-2 and cellular inhibitor of apoptosis-1 (cIAP) and cIAP-2, which function in an additive fashion to protect cells from TNF-induced injury (45). Bcl-2, Bcl-XL, and FLICE-inhibitor protein (cFLIP) might also confer protection (46). In the future, it will be important to determine how TNF regulates these anti-apoptotic proteins in microglia versus oligodendrocytes.

Our study examined the consequences of divergent patterns of TNF receptor expression in microglia and OL in vitro. It is important to consider receptor expression and responses to TNF by these cells in vivo. Mature OL are neuroectodermally-derived stationary cells that extrude, concentrically wrap, and compact

myelin, myelinating up to 50 axons per cell. In contrast, amoeboid microglia are mobile phagocytic cells that secrete proteases, oxyradicals (e.g., NO, $\cdot\text{O}_2^-$), and proinflammatory cytokines which can directly injure OL. Like peripheral macrophages, microglia secrete TNF as part of a defensive armamentarium, necessitating the development of mechanisms to protect them from TNF-induced apoptosis and necrosis. In the absence of disease, mature myelinating OL are not normally exposed to TNF and may not be equipped to neutralize its harmful effects. Interestingly, a recent report using knockout mice indicates that signals delivered through TNFR2 stimulate the proliferation of oligodendrocyte progenitors following cuprizone-induced demyelination (47). It will therefore be important to determine the pattern of TNFR1 and TNFR2 expression and the details of TNF-induced signaling in OL during different phases of inflammation associated with multiple sclerosis and its animal models.

ACKNOWLEDGMENTS

We thank Dr. Stephanie Liva for helpful suggestions on an earlier draft of this paper, Mr. Soheil Simzar for help with Western blots, and Ms. Ruth Cole for expertise in preparing primary culture of glial cells. This research was supported by National Multiple Sclerosis Society grant RG 2751-A-1 and NICHD grant HD06576.

REFERENCES

- Hofman, F., Hinton, D., Johnson, K., and Merrill, J. 1989. Tumor necrosis factor identified in multiple sclerosis brain. *J. Exp. Med.* 170:607–612.
- Selmaj, K., Raine, C., Canella, B., and Brosnan, C. 1991. Identification of lymphotoxin and tumor necrosis factor in multiple sclerosis lesions. *J. Clin. Invest.* 87:949–954.
- Kuroda, T. and Simamoto, Y. 1991. Human tumor necrosis factor- α augments experimental allergic encephalomyelitis in rats. *J. Neuroimmunol.* 34:159–164.
- Ruddle, N., Bergman, C., McGrath, K., Lingenheld, E., Grunnet, M., Padula, S., and Clark, R. 1990. An antibody to lymphotoxin and tumor necrosis factor prevents transfer of experimental allergic encephalomyelitis. *J. Exp. Med.* 172:1193–1200.
- Selmaj, K., Raine, C., and Cross, A. 1991. Anti-tumor necrosis factor therapy abrogates autoimmune encephalomyelitis. *Ann. Neurol.* 30:694–700.
- Selmaj, K., Papierz, W., Glabinski, A., and Kono, T. 1995. Prevention of chronic relapsing experimental autoimmune encephalomyelitis by soluble tumor necrosis factor receptor I. *J. Neuroimmunol.* 56:135–141.
- Merrill, J. 1991. The effects of IL-1 and TNF α on astrocytes, microglia, oligodendrocytes, and glial precursors in vitro. *Dev. Neurosci.* 13:130–137.
- Selmaj, K., Farooq, M., Norton, W., Raine, C., and Brosnan, C. 1990. Proliferation of astrocytes in vitro in response to cytokines. A primary role for tumor necrosis factor. *J. Immunol.* 144:129–135.
- Kahn, M., Ellison, J., Speight, G., and de Vellis, J. 1995. CNTF regulation of astrogliosis and the activation of microglia in the developing rat central nervous system. *Brain Res.* 685:55–67.
- Giulian, D. and Ingerman, J. 1988. Colony-stimulating factors as promoters of amoeboid microglia. *J. Neurosci.* 8:4707–4717.
- Théry, C. and Mallat, M. 1993. Influence of interleukin-1 and tumor necrosis factor alpha on the growth of microglial cells in primary cultures of mouse cerebral cortex: involvement of colony stimulating factor 1. *Neurosci. Lett.* 150:195–199.
- Dopp, J., MacKenzie-Graham, A., Otero, G., and Merrill, J. 1997. Differential expression, cytokine modulation, and specific functions of type-1 and type-2 tumor necrosis factor receptors in rat glia. *J. Neuroimmunol.* 75:104–112.
- Merrill, J., Ignarro, L., Sherman, M., Melinek, J., and Lane, T. 1993. Microglial cell cytotoxicity of oligodendrocytes is mediated through nitric oxide. *J. Immunol.* 151:2132–2141.
- McLarnon, J., Michikawa, M., and Kim, S. 1993. Effects of tumor necrosis factor on inward potassium current and cell morphology in cultured human oligodendrocytes. *Glia* 9:120–126.
- Soliven, B. and Szuchet, S. 1995. Signal transduction pathways in oligodendrocytes: Role of tumor necrosis factor- α . *Int. J. Dev. Neurosci.* 13:351–367.
- Selmaj, K. and Raine, C. 1988. Tumor necrosis factor mediates myelin and oligodendrocyte damage in vitro. *Ann. Neurol.* 23:339–346.
- Selmaj, K., Raine, C., Farooq, M., Norton, W., and Brosnan, C. 1991. Cytokine cytotoxicity against oligodendrocytes: Apoptosis induced by lymphotoxin. *J. Immunol.* 147:1522–1529.
- Gossens, V., Grooten, J., De Vos, K., and Fiers, W. 1995. Direct evidence for tumor necrosis factor-induced mitochondrial reactive oxygen intermediates and their involvement in cytotoxicity. *Proc. Natl. Acad. Sci. USA* 92:8115–8119.
- Green, D. and Reed, J. 1998. Mitochondria and apoptosis. *Science* 281:1309–1312.
- Chae, H. Z., Kang, S. W., and Rhee, S. G. 1999. Isoforms of mammalian peroxiredoxin that reduce peroxides in presence of thioredoxin. *Methods in Enzymology* 300:219–226.
- Netto, L. S., Chae, H. Z., Kang, S. W., Rhee, S. G., and Stadtman, E. R. 1996. Removal of hydrogen peroxide by thiol-specific antioxidant enzyme (TSA) is involved with its antioxidant properties. *J. Biol. Chem.* 271:15315–15321.
- Sauri, H., Butterfield, L., Kim, A., and Shau, H. 1995. Antioxidant function of recombinant human natural killer enhancing factor. *Biochem. Biophys. Res. Comm.* 208:964–969.
- Shau, H., Merino, A., Chen, L., Shih, C. C.-Y., and Colquhoun, S. D. 2000. Induction of peroxiredoxins in transplanted livers and demonstration of their in vitro cytoprotection activity. *Antioxidants and Redox Signaling* 2:347–354.
- Zhang, P., Liu, B., Kang, S. W., Seo, M. S., Rhee, S. G., and Obeid, L. M. 1997. Thioredoxin peroxidase is a novel inhibitor of apoptosis with a mechanism distinct from that of Bcl-2. *J. Biol. Chem.* 272:30615–30618.
- Siow, R. C., Ishii, T., Sato, H., Taketani, S., Leake, D. S., Sweiry, J. H., Pearson, J. D., Bannai, S., and Mann, G. E. 1995. Induction of the antioxidant stress proteins heme oxygenase-1 and MSP23 by stress agents and oxidised LDL in cultured vascular smooth muscle cells. *Febs Letters* 368:239–242.
- Kim, A. T., Sarafian, T. A., and Shau, H. 1997. Characterization of antioxidant properties of natural killer-enhancing factor-B and induction of its expression by hydrogen peroxide. *Toxicol. Applied Pharm.* 147:135–142.
- Sarafian, T., Huang, C., Kim, A., de Vellis, J., and Shau, H. 1998. Expression of the antioxidant gene NKEF in the central nervous system. *Molec. Chem. Neuropath.* 34:39–51.
- Sarafian, T. A., Verity, M. A., Vinters, H. V., Shih, C. C.-Y., Shi, L., Ji, X. D., Dong, L., and Shau, H. 1999. Differential expression of peroxiredoxin subtypes in human brain cell types. *J. Neurosci. Res.* 56:206–212.
- Thorburne, S. and Juurlink, B. 1996. Low glutathione and high

- iron govern the susceptibility of oligodendroglia precursors to oxidative stress. *J. Neurochem.* 67:1014–1022.
30. Back, S., Gan, X., Li, Y., Rosenberg, P., and Volpe, J. 1998. Maturation-dependent vulnerability of oligodendrocytes to oxidative stress-induced death caused by glutathione depletion. *J. Neurosci.* 18:6241–6253.
 31. Cole, R. and de Vellis, J. 1989. Preparation of astrocyte and oligodendrocyte cultures from primary rat glial cultures, in *A Dissection and Tissue Culture Manual of the Nervous System* (Shahar, A., de Vellis, J., Vernadakis, A., and Haber, B., eds), pp. 121–133. Alan R. Liss, New York.
 32. Bass, D. A., Parce, J. W., Dechatelet, L. R., Szejda, P., Seeds, M. C., and Thomas, M. 1983. Flow cytometric studies of oxidative product formation by neutrophils: A graded response to membrane stimulation. *J. Immunol.* 130:1910–1917.
 33. Possel, H., Noack, H., Augustin, W., Keilhoff, G., and Wolf, G. 1997. 2,7-dihydrodichlorofluorescein diacetate as a fluorescent marker for peroxynitrite formation. *FEBS Lett.* 416:175–178.
 34. Cook, J., Pass, H., Iype, S., Friedman, N., DeGraff, W., Russo, A., and Mitchell, J. 1991. Cellular glutathione and thiol measurements from surgically resected human lung tumor and normal lung tissue. *Cancer Res.* 46:6105–6110.
 35. Sarafian, T., Vartavarian, L., Kane, D., Bredesen, D., and Verity, A. (1994). Bcl-2 expression decreases methyl mercury-induced free-radical generation and cell killing in a neural cell line. *Toxicology Lett.*, 74:149–155.
 36. Shau, H., Gupta, R. K., and Golub, S. H. 1993. Identification of a natural killer enhancing factor NKEF from human erythroid cells. *Cell. Immunol.* 147:1–11.
 37. Shau, H. and Kim, A. 1994. Identification of natural killer enhancing factor as a major antioxidant in human red blood cells. *Biochem. Biophys. Res. Com.* 199:83–88.
 38. Hsu, H., Shu, H., Pan, M., and Goeddel, D. 1996. TRADD-TRAF2 and TRADD-FADD interactions define two distinct TNF receptor 1 signal transduction pathways. *Cell* 84:299–308.
 39. Rothe, M., Wong, S., Henzel, W., and Goeddel, D. 1994. A novel family of putative signal transducers associated with the cytoplasmic domain of the 75 kDa tumor necrosis factor receptor. *Cell* 78:681–692.
 40. Hisahara, S., Shoji, S., Okano, H., and Miura, M. 1997. ICE/CED-3 family executes oligodendrocyte apoptosis by tumor necrosis factor. *J. Neurochem.* 69:10–20.
 41. Wong, G. and Goeddel, D. 1988. Induction of manganous superoxide dismutase by tumor necrosis factor: Possible protective mechanism. *Science* 242:941–944.
 42. Pinteaux, E., Perraut, M., and Tholey, G. 1998. Distribution of mitochondrial manganese superoxide dismutase among rat glial cells in culture. *Glia* 22:408–414.
 43. Schulze-Osthoff, K., Beyaert, R., Vandevoorde, V., Haegeman, G., and Fiers, W. 1993. Depletion of the mitochondrial electron transport abrogates the cytotoxic and gene-inductive effects of TNF. *EMBO Journal*, 12:3095–3014.
 44. Antwerp, D., Martin, S., Kafri, T., Green, D., and Verma, I. 1996. Suppression of TNF- α -induced apoptosis by NF- κ B. *Science* 274:787–789.
 45. Wang, C.-Y., Mayo, M., Korneluk, R., Goeddel, D., and Baldwin, A. 1998. NF- κ B antiapoptosis: Induction of TRAF1 and TRAF2 and c-IAP1 and c-IAP2 to suppress caspase-8 activation. *Science* 281:1680–1683.
 46. Kreuz, S., Siegmund, D., Scheurich, P., and Wajant, H. 2001. NF- κ B inducers upregulate cFLIP, a cyclohexamide-sensitive inhibitor of death receptor signaling. *Molec. Cell. Bio.* 21:3964–3973.
 47. Arnett, H., Mason, J., Marino, M., Suzuki, K., Matsushima, G., and Ting, J. 2001. TNF α promotes proliferation of oligodendrocyte progenitors and remyelination. *Nat. Neurosci.* 4:1116–1122.